ACS OMEGA

Article

Cite This: ACS Omega 2018, 3, 6770−6778

Nanotoxicity of Silver Nanoparticles on HEK293T Cells: A Combined Study Using Biomechanical and Biological Techniques

Xuefeng Jiang,[†,‡,§,∥] Chunjiao Lu,[†,‡,∥] Mingjie Tang,[†,§] Zhongbo Yang,[†,§] Weijiao Jia,[†,‡,§] Yanbo Ma,[†] Panpan Jia,[†,‡] Desheng Pei,*[,†,‡] and Huabin Wang*[,†,‡,§]

[†]Chongqing Institute of Green and Intelligent Technology, Chinese Academy of Sciences, Chongqing 400714, China

[‡]University of Chinese Academy of Sciences, Beijing 100049, China

[§]Chongqing Engineering Research Center of High-Resolution and Three-Dimensional Dynamic Imaging Technology, Chongqing 400714, China

ABSTRACT: Human embryonic kidney 293T cells (HEK293T cells) before and after treatment with silver nanoparticles (AgNPs) were measured using advanced atomic force microscopy (AFM) force measurement technique, and the biomechanical property of cells was analyzed using a theoretical model. The biomechanical results showed that the factor of viscosity of untreated HEK293T cells reduced from 0.65 to 0.40 for cells exposure to 40 μg/mL of AgNPs. Comet assay indicated that significant DNA damage occurred in the treated cells, measured as tail DNA% and tail moment. Furthermore, gene expression analysis showed that for the cells treated with 40 μg/mL of AgNPs, the antiapoptosis genes *Bcl2-t* and *Bclw* were, respectively, downregulated to 0.65- and 0.66-fold of control, and that the proapoptosis gene *Bid* was upregulated to 1.55-fold of control, which indicates that apoptosis occurred in cells exposed to AgNPs. Interestingly, excellent negative correlations were found between the factor of viscosity and tail DNA%, and tail moment, which suggest that the biomechanical property can be correlated with genotoxicity of nanoparticles on the cells. Based on the above results, we conclude that (1) AgNPs can lead to biomechanical changes in HEK293T cells, concomitantly with biological changes including cell viability, DNA damage, and cell apoptosis; (2) the factor of viscosity can be exploited as a promising label-free biomechanical marker to assess the nanotoxicity of nanoparticles on the cells; and (3) the combination of AFM-based mechanical technique with conventional biological methods can provide more comprehensive understanding of the nanotoxicity of nanoparticles than merely by using the biological techniques.

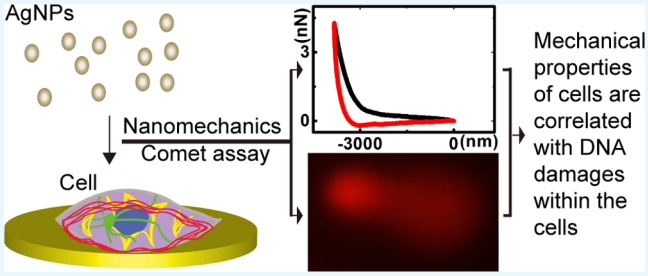

1. INTRODUCTION

Nanoparticles (NPs) have attracted tremendous interest of scientists due to their unique properties including large surface area, small size, special surface chemistry, etc.[1] As a result, various NPs, for example, silver-, gold-, and silica-based NPs have been synthesized in past decades for different applications such as drug delivery, cancer diagnostics and therapy, and antiseptic sprays and bandages.[2−4] Almost simultaneously, the biosafety of NPs has also been receiving increasing attention by the scientific communities, with the wide applications of NPs contained products and devices.[5−7] Consequently, the effects of NPs on eukaryotic cells have been intensively investigated, mainly with fluorescence-based detection techniques such as 3-(4,5-dimethylthiazol-2-yl)-2,5-diphenyltetrazolium bromide (MTT) test, comet assay, polymerase chain reaction (PCR), flow cytometry, and fluorescence microscopy, to examine cell viability, DNA damage, gene expression, etc.[8−11] Indeed, it has been found that many NPs have toxicity to cells and can lead to cell death or change in cell state, normally in a dose-dependent manner.[12−14] Although significant information has been obtained using these biological techniques in terms the toxicity of NPs, the molecules within or extracted from the cells are usually required to be labeled specifically for the detection in these biological techniques, which can lead to high cost, time consumption, false positive or negative results, etc.

With the rapid development of nanotechnology, there has been an increasing consensus that cell state can not only be evaluated by using biological techniques but also be examined using biomechanical techniques, particularly atomic force microscopy (AFM)-based force measurement techniques.[15−19] AFM is a powerful tool for the mechanical measurement of living cells in near-physiological conditions and can be employed to study the biological processes and functions of cells from the perspective of mechanics. For example, the biological response of influx of Ca^{2+} into the human neuroblastoma SH-SY5Y cells triggered by the opening of ligand-gated ion channels could be examined using AFM-based mechanical measurements.[20] More recently, we used the factor of viscosity to evaluate the action of an anticancer drug (docetaxol) on HeLa cells and found that docetaxol-treated

Received: March 29, 2018
Accepted: June 6, 2018
Published: June 21, 2018

DOI: 10.1021/acsomega.8b00608
ACS Omega 2018, 3, 6770−6778

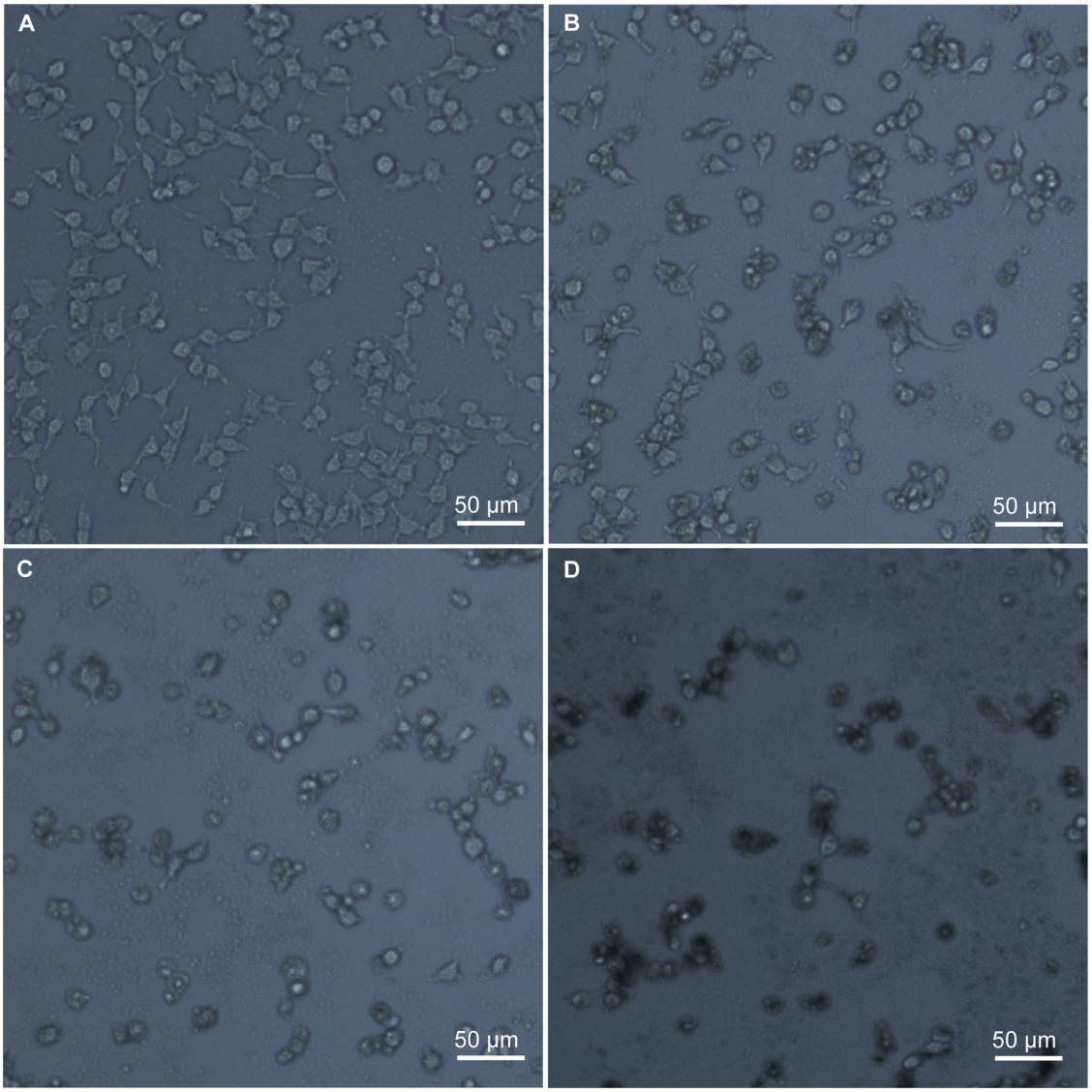

Figure 1. Representative images of HEK293T cells following exposure to varying AgNPs concentrations for 24 h, observed using an inverted optical microscope: (A) 0 μg/mL, (B) 10 μg/mL, (C) 20 μg/mL, and (D) 40 μg/mL.

cells had a smaller factor of viscosity than the untreated cells.[18] These studies demonstrated that the mechanical properties of cells are very sensitive to the cell state/functional change, strongly implicating that the influence of NPs on cells could be examined using AFM-based mechanical measurements. Compared to those fluorescence-based techniques, the AFM-based biomechanical techniques are label-free and can assess the cell state from the perspective of mechanics. Therefore, AFM-based biomechanical techniques are promising for the evaluation of the toxicity of NPs on cells. The combination of AFM biomechanical measurement with biological techniques should be able to provide more comprehensive insights into the toxicity of NPs on cells than only by using biological methods, which is critical for accurately assessing the biosafety of NPs. Silver nanoparticles (AgNPs) have been reported as promising antibacterial agents and tumor inhibitors, and the toxicity of AgNPs has been investigated intensively in recent years.[21−23] However, little work has been carried out to evaluate the toxicity of AgNPs on cells from the perspective of biomechanics, which impedes our comprehensive understanding of the nanotoxicity of AgNPs.

The human embryonic kidney 293T cell (HEK293T) is a cell line derived from the human embryonic kidney cell and has been widely used as the model cell in the studies of NPs' toxicity.[24] In the present work, we aimed to interrogate the nanotoxicity of NPs on eukaryotic cells by employing a sophisticated AFM-based biomechanical technique, and explored the influence of AgNPs on HEK293T cells. The toxicity of AgNPs on HEK293T cells was also investigated biologically using the MTT assay, single cell gel electrophoresis, and quantitative real-time polymerase chain reaction (qRT-PCR) to examine the cell viability, DNA damage, and gene expression, respectively. The mechanical data showed that the factor of viscosity of cells was significantly decreased from 0.65 for untreated cells to 0.40 for the cells treated with 40 μg/mL of AgNPs. The biological results indicated that AgNPs exposure decreased cell viability, increased DNA damage, downregulated *Bcl-2t* and *Bclw* genes, and upregulated the *Bid* gene. *Bcl-2t* and *Bclw* are antiapoptosis genes, whereas *Bid* is a proapoptosis gene.[11,25,26] Interestingly, the factor of viscosity was found to be negatively correlated with the DNA damage measured as tail DNA% and tail moment. The work demonstrated here suggests

DOI: 10.1021/acsomega.8b00608
ACS Omega 2018, 3, 6770−6778

that AFM-based biomechanical measurement can provide researchers a physical and label-free means to assess the nanotoxicity of NPs on cells, and that the combination of the mechanical technique with biological methods can provide a more comprehensive understanding of the nanotoxicity of NPs on cells than merely by using biological techniques.

2. RESULTS AND DISCUSSION

2.1. Cell Viability Test. The optical microscopic images of HEK293T cells upon treatment with AgNPs are shown in Figure 1. From Figure 1A, it can be seen that HEK293T cells without exposure to AgNPs (control) show a spindle shape, which is typical for untreated HEK293T cells.[8,27] However, the cells treated with AgNPs present clear alterations in both morphology and number (Figure 1B,C), i.e., the cells tended to turn into a roundish shape and the cell density gradually decreased with increasing concentration of AgNPs, similar to the effect of graphene oxide sheets on HEK293T cells and other drugs or NPs on HeLa cells and/or MDA-MB-231 cells.[8,18,28] The morphological and inhibitory changes indicated that AgNPs are cytotoxic to HEK293T cells.

To further confirm this, the cell viability was assessed using the MTT assay and quantified according to eq 1. Compared to the control group, the treated HEK293T cells indeed showed decreased viability with increasing concentration of AgNPs and the cell viability was about 69.07% of the control when the concentration of AgNPs reached 40 μg/mL (Figure 2). This

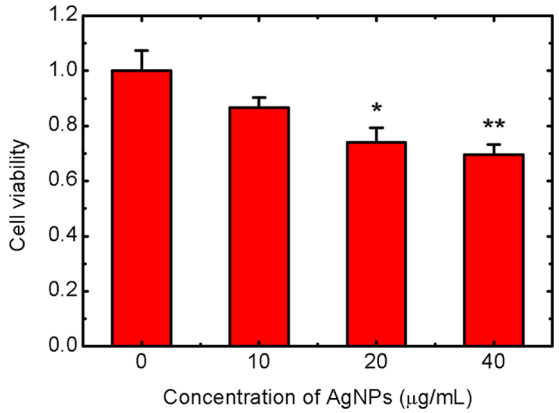

Figure 2. Cell viability of HEK293T cells tested by the MTT assay. HEK293T cells were treated with varying AgNPs concentrations (0, 10, 20, and 40 μg/mL) for 24 h. Following treatment with MTT reagents, viable cells were quantified by measuring the OD_{490} of sample wells. * indicates $p < 0.05$ and ** indicates $p < 0.01$.

trend is consistent with the previous studies that the cytotoxicity of AgNPs on HeLa cells, U937 cells, and HCT116 cells is dose-dependent and increases with the concentration of AgNPs in a certain range.[29,30]

2.2. Mechanical Property of HEK293T Cells. The effects of AgNPs on HEK293T cells were evaluated by measuring the cellular mechanical properties using an AFM force measurement technique. From the force versus distance curve, the factor of viscosity, φ, can be obtained according to eq 2. As shown in Figure 3, the viscous energy, originating from the energy dissipation in the process of deforming the cell, is the hysteresis between the approach and retraction curves, indicated by the yellow area encompassed by the approach curve, retraction curve, and zero-force line. The elastic energy is

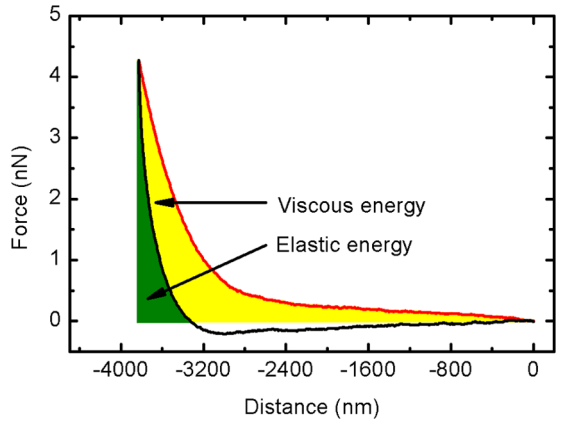

Figure 3. Biomechanical analysis of HEK293T cells in phosphate buffer solution (PBS) buffer. A sample force versus distance curve obtained on an untreated HEK293T cell shows the tip approach (red) and withdrawal (back). The energy involved in the indentation process includes two parts: elastic energy (green) and viscous energy (yellow).

the energy for the cellular deformation recovery, indicated by the green area formed by the positive portion of the retraction force curve and the zero-force line. The factor of viscosity is equal to the ratio of the viscous energy to the total energy (the summation of the viscous energy and the elastic energy) exerted on the cell in the process of deforming the cell. Previous studies have suggested that the factor of viscosity is a much more meaningful physical parameter than the usually used Young's modulus obtained by the Hertz−Sneddon model because cells are viscoelastic materials and, strictly speaking, cannot be modeled as an ideal elastic body using the Hertz−Sneddon model.[18]

The calculated factor of viscosity of the cells treated with varying concentrations of AgNPs (0, 10, 20, and 40 μg/mL) was plotted to a histogram, respectively (Figure 4A−D). For each concentration, more than 300 curves were measured and calculated to obtain the factor of viscosity. The plots were fitted to Gaussian function to obtain the mean value of the factor of viscosity that is summarized in Table 1. As shown in Figure 4D and Table 1, the factor of viscosity for the cells treated with 40 μg/mL AgNPs has two values, i.e., 0.42 (peak #1) and 0.60 (peak #2), indicating that the cells can be roughly categorized into two different groups, i.e., cells strongly influenced by AgNPs and cells tolerant to AgNPs. In fact, the morphology of the cells has been observed to be uneven from the optical microscopy image (Figure 1D), which also indicates that cells with different states exist on the sample, likely due to the response of cell heterogeneity on nanoparticle dose.[31,32] Cells with different morphologies were also observed for HeLa cells and MDA-MB-231 cells treated with selenium nanoparticles.[28] Because individual cells were randomly targeted in AFM force measurement, cells with different states could be measured; as a result, the calculated factor of viscosity has more than one value.

Compared to 0.65 of the control, the factor of the viscosity of cells after AgNPs exposure was decreased to 0.64 for 10 μg/mL, 0.54 for 20 μg/mL, and 0.42 (peak #1) for 40 μg/mL. The values of 0.54 and 0.42 are significantly different from 0.65 for the control. These results mean that the influence of AgNPs on HEK293T cells can be detected mechanically. Considering both MTT test (Figure 2) and calculated factor of viscosity (Table 1), it is clear that the lower the cell viability, the lower

DOI: 10.1021/acsomega.8b00608
ACS Omega 2018, 3, 6770−6778

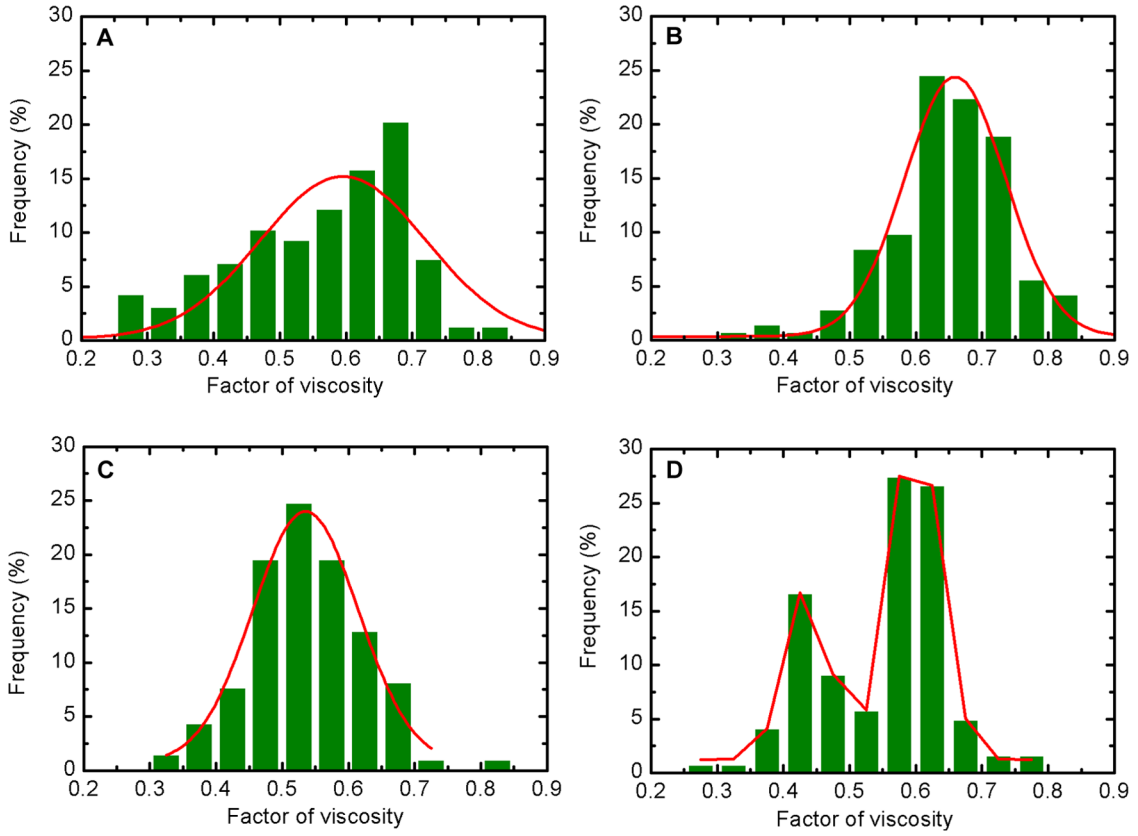

Figure 4. Gaussian fitting of the factor of viscosity for HEK293T cells. The cells were treated with (A) 0 μg/mL, (B) 10 μg/mL, (C) 20 μg/mL, and (D) 40 μg/mL AgNPs for 24 h, respectively.

Table 1. Statistics of the Factor of Viscosity for HEK293T Cells Treated with Varying AgNPs Concentrations[a]

AgNPs concentration (μg/mL)	factor of viscosity
0 (control)	0.65 ± 0.02
10	0.64 ± 0.01
20	0.54 ± 0.01*
40	0.42 ± 0.01 (peak #1)**
	0.60 ± 0.01 (peak #2)

[a]* Indicates $p < 0.05$ and ** indicates $p < 0.01$.

the factor of viscosity. From its definition, it is easy to understand that the lower the factor of viscosity, the higher the relative cellular elasticity (related to higher elastic energy).

It has been well recognized that biomechanical changes are connected to the cytoskeletal alterations.[33,34] In a recent study, Huang et al. found that the shape of human dermal fibroblasts was changed from a normal spindle to a triangle when the cells were exposed to AgNPs for a long time, concomitantly with partial cytoskeletal contraction and actin filament rearrangement along the cell periphery.[35] In our present work, the changes in the cellular morphology such as shape and size with the increase in AgNPs concentration (see Figure 1) also strongly indicate the alterations of cytoskeleton, which should be mainly responsible for the biomechanical changes of the cells, measured by the variation in the factor of viscosity. However, because NPs−cytoskeleton interaction is a new research area, the underlying mechanisms regarding the influence of NPs on cytoskeleton change and the contribution of cytoskeleton change to cellular mechanical properties are still unclear and imperative to be further investigated by the scientific community to fully understand the cytotoxicity of NPs.

2.3. DNA Damage. The toxicity of AgNPs on HEK293T cells was further studied using comet assay, which is a robust method to perform genotoxicity measurements.[36] It can be seen from Figure 5 that the comet tail becomes more evident with increasing concentration of AgNPs, as compared to the comet head, indicating higher levels of DNA damage in the cells. The percentage of DNA in the comet tail (tail DNA%) and tail moment were two preferable parameters used to quantify DNA damages.[37,38] Tail DNA% is defined as 100× comet tail DNA intensity/whole cell DNA intensity, whereas tail moment equals tail DNA% × length of comet tail. The statistical results of tail DNA% and tail moment are presented in Table 2. The parameters are significantly increased after the cell exposure to AgNPs (10, 20, and 40 μg/mL) for 24 h, in comparison with the control.

More interestingly, significant dose response trends were found for both the tail DNA% and the tail moment using linear regression (Figure 6). The goodness of fit (adj. R^2) was very high for the samples exposed to different doses of AgNPs. In recent studies, it was found that the DNA damage measured as tail DNA% in coelomocytes of earthworms appeared as a positive linear response to the dose of γ radiation,[37] and that the DNA damage in peripheral blood leukocytes of different groups of mice showed a linear gradual increase with age.[39] In this work, we also found that the DNA damage in HEK293T cells caused by AgNPs can be evaluated using tail DNA% and tail moment, and that the two parameters linearly increase with the concentration of AgNPs.

DOI: 10.1021/acsomega.8b00608
ACS Omega 2018, 3, 6770−6778

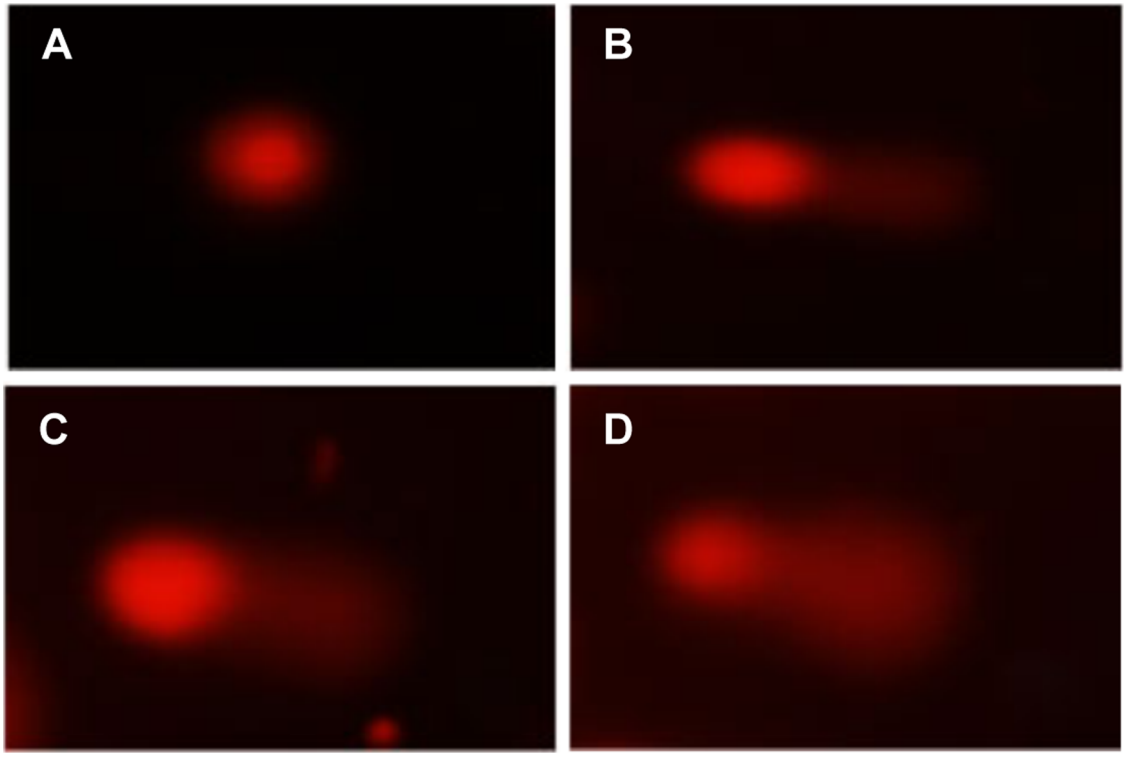

Figure 5. Images of DNA damages detected by comet assays for HEK293T cells treated with varying AgNPs concentrations for 24 h: (A) 0 μg/mL, (B) 10 μg/mL, (C) 20 μg/mL, and (D) 40 μg/mL.

Table 2. DNA Damage in HEK293T Cells Induced by Varying AgNPs Concentrations[a]

AgNPs concentration (μg/mL)	tail DNA%	tail moment
0 (control)	1.1 ± 0.6	0.6 ± 0.3
10	15.1 ± 2.5***	18.6 ± 4.5*
20	35.6 ± 2.4***	51.1 ± 5.7***
40	55.3 ± 2.1***	89.7 ± 6.1***

[a]* Indicates $p < 0.05$, ** indicates $p < 0.01$ and *** indicates $p < 0.001$.

2.4. mRNA Expression Profiles of Selected Genes. To deeply understand the mechanisms of the action of AgNPs on HEK293T cells, several key genes, including antiapoptotic *Bcl2-t* and *Bclw* genes and proapoptotic *Bid* gene, were analyzed using qRT-PCR (Figure 7). The results showed that *Bcl2-t* expression levels reduced significantly to 0.57-, 0.63-, and 0.65-fold of the control level, respectively, after the cell exposure to 10, 20, and 40 μg/mL AgNPs for 24 h. Under the same treatment, the expression levels of *Bclw* were decreased to 0.9-, 0.78-, and 0.66-fold of the control level, whereas those of *Bid* were upregulated to 1.31-, 1.38-, and 1.55-fold of the control level. After exposure to AgNPs (40 μg/mL), *Bclw* was significantly downregulated, whereas *Bid* was significantly upregulated. The data strongly suggested that AgNPs induced apoptosis in HEK293T cells at a high AgNPs concentration (40 μg/mL),[11,14] consistent with the fact that AgNPs can induce HePG-2 cells apoptosis.[12]

2.5. Correlation between the Biomechanics with DNA Damage. In this work, the factor of viscosity was used as a biomarker to evaluate the influence/toxicity of AgNPs on cells. On the other hand, the DNA damage was also investigated after the cell exposure to AgNPs by using the widely accepted comet assay. To understand the biological origin of the biomechanical change, it is important to see whether or not the factor of viscosity can be correlated to the DNA damage. To do this, the correlation between the change of factor of viscosity and the change of tail DNA%, and the change of tail moment was analyzed using Origin 8.5 software, respectively. It was found the correlation coefficient (Pearson coefficient) for the change of factor of viscosity and the change of tail DNA% is −0.99 ($p < 0.05$) and that for the change of factor of viscosity and the change of tail moment is −0.99 ($p < 0.005$). It is a very interesting result because the mechanical data are highly negatively correlated with the biological data, indicating that the mechanical properties might be closely related with the DNA damage and that the factor of viscosity can be employed as an effective label-free biomechanical marker to assess the cytotoxicity of NPs. To our knowledge, the mechanical properties of the cells were first found to be well correlated with the DNA damage in cells upon exposure to NPs.

3. CONCLUSIONS

In summary, the factor of viscosity calculated from the AFM biomechanical measurements was introduced to investigate the biomechanical properties of the cells with or without treatment with AgNPs. In addition, conventional biological techniques including MTT test, comet assay, and gene expression analysis were employed to evaluate the cytotoxicity and genotoxicity of AgNPs. The biomechanical results showed that the factor of viscosity was reduced with increasing AgNPs concentrations, indicating that cellular structural changes occurred upon treatment with AgNPs. Biological results demonstrated decreased cell viability, increased DNA damage, downregulated antiapoptosis *Bcl2-t* and *Bclw* genes, and upregulated proapoptosis *Bid* gene for the cells exposure to AgNPs with increasing concentrations. Most importantly, it was discovered

DOI: 10.1021/acsomega.8b00608
ACS Omega 2018, 3, 6770−6778

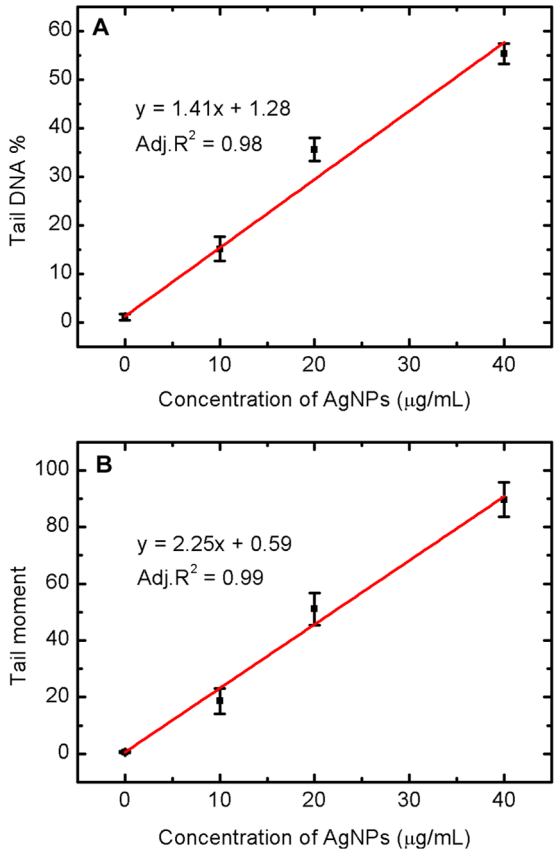

Figure 6. Dose−response relationship for DNA damage in HEK293T cells after exposure to AgNPs measured using the comet assay. DNA damage in terms of (A) tail DNA% and (B) tail moment obtained at different AgNPs concentrations (0, 10, 20, and 40 μg/mL), fitted each with a linear regression line.

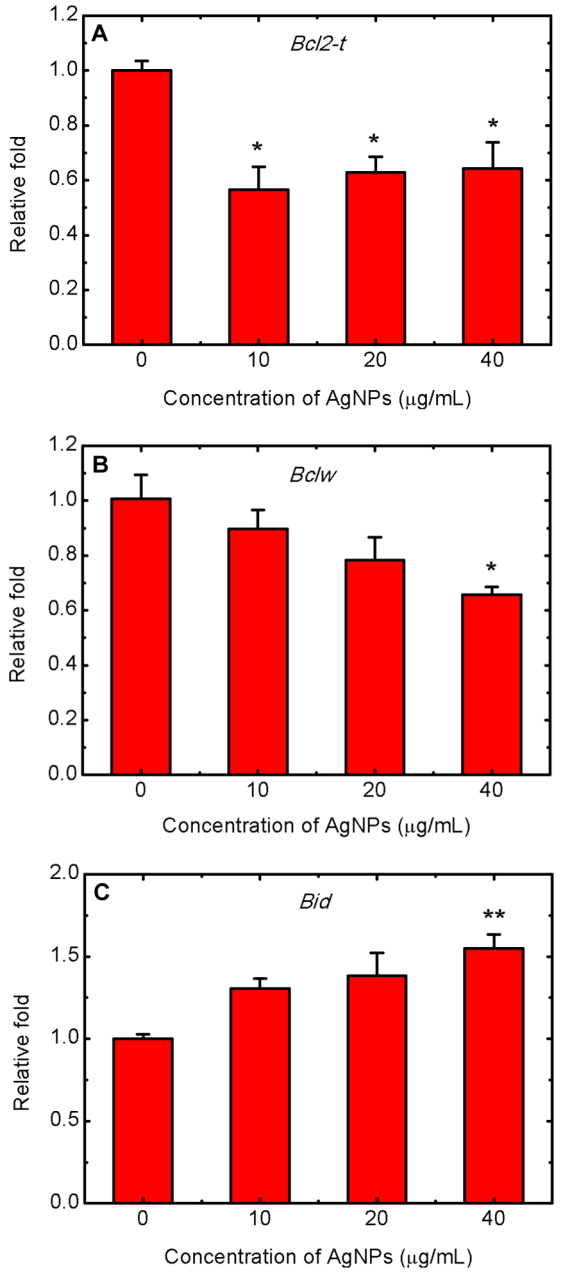

Figure 7. Gene expression levels for HEK293T cells after exposure to varying AgNPs concentrations (0, 10, 20, and 40 μg/mL) for 24 h: (A) *Bcl2-t*, (B) *Bclw*, and (C) *Bid*. * indicates $p < 0.05$ and ** indicates $p < 0.01$.

that the factor of viscosity can be well correlated with DNA damage, corroborating the effectiveness of using a biomechanical marker (the factor of viscosity) to assess the nanotoxicity of AgNPs. It needs to pointed out that the nanotoxicity of AgNPs at high concentrations in the cells is worthy of further investigation by developing suitable biocompatible surface modification techniques that enable the attachment of cells treated with high concentration AgNPs on a substrate for the AFM force measurement. Taken together, the findings in our present work demonstrated that the biomechanical technique can be used as a very useful means in the study of nanotoxicity of NPs from the mechanical perspective, and that the combination of AFM-based mechanical techniques with biological means can help us obtain more comprehensive insights into the toxicity of NPs than just by using biological techniques.

4. MATERIALS AND METHODS

4.1. AgNPs Solutions. AgNPs (CAS No. 7440-22-4, particle size ∼60 nm measured by transmission electron microscopy, 99% trace metals basis) were purchased from Sigma-Aldrich (Shanghai, China). The AgNPs powder was suspended in Milli-Q water (18.2 MΩ/cm, Millipore, Billerica, MA) and sonicated at 50 W/L, 40 kHz for 50 min to prepare the stock solution (1 mg/mL). The surface charge of AgNPs was ∼−40 mV, measured by a Zetasizer Nano ZS apparatus (Malvern Instruments Ltd., Malvern, U.K.). The stock solution was freshly prepared every 24 h to keep the quality consistent and further diluted into cell culture media to the desired AgNPs concentrations (10, 20, and 40 mg/L) before the cell exposure experiments.

4.2. Cells Culture and Cell Viability Measurement. HEK293T cells (American Type Culture Collection, CRL-11268, Shanghai, China) were cultured in Gibco Roswell Park Memorial Institute medium 1640 basic (1×) supplemented with 10% fetal bovine serum (Gibco, Thermo Fisher Scientific, Shanghai, China) and 1% penicillin−streptomycin solution (Beyotime, Jiangsu, China) at 37 °C in an incubator humidified with 5% CO_2 atmosphere.

The cells were seeded in 96-well plates (100 μL/well) with a density of ∼1 × 10^4 cells/well and grown for 12 h at 37 °C.

DOI: 10.1021/acsomega.8b00608
ACS Omega 2018, 3, 6770−6778

Then, the medium was removed and the cells were washed twice with phosphate buffer solution (PBS, HyClone, Beijing, China). Afterward, the cells were exposed to different concentrations of AgNPs solutions (10, 20, and 40 μg/mL) by adding 100 μL AgNPs solution to each well. The media containing no AgNPs were used as control. The cells were then grown for a further 24 h at 37 °C.

The viability of the cells after exposure to AgNPs was analyzed using a cell proliferation kit (MTT, Sigma-Aldrich, Shanghai, China). Briefly, 10 μL of 5 mg/mL MTT solution in the PBS buffer was added to each well and the cells were allowed to grow for another 4 h. The MTT-containing medium was removed and the cells were then treated by adding 100 μL of dimethyl sulfoxide to each well to dissolve the formazan crystal formed by live cells. The plates were then transferred to a microplate reader (Epoch, BioTek Instruments Inc., Shoreline, WA) and the absorbance (optical density (OD)) value of the wells was measured at a wavelength of 490 nm according to the manufacturer's instruction. The data for each condition represents the average values taken from three replicate wells performed in three independent experiments. The measured absorbance value (OD) of the wells was used to calculate the inhibition rate, via the formula

$$\text{inhibition rate} = \frac{(\text{OD}_{\text{control well}} - \text{OD}_{\text{experimental well}})}{\text{OD}_{\text{control well}}} \times 100\% \quad (1)$$

Upon the completion of the MTT assay, the cell morphology was examined by observing the plates using an inverted optical microscope (Olympus Corporation, Tokyo, TH4-200, Japan).

4.3. Nanomechanical Measurement and Analysis of HEK293T Cells Using AFM. For mechanical measurements, 3 mL of HEK293T cell solution (~1×10^5 cells/mL) was seeded in a Petri dish (60 mm × 15 mm, Corning Inc., New York, NY) coated with poly-L-lysine and the cells were cultured for 12 h at 37 °C at 5% CO_2. The supernatant was removed and the cells were washed with PBS twice. Afterward, the cells were exposed to different concentrations of AgNPs (10, 20, and 40 μg/mL) or cell culture media (control) by adding 3 mL solution to each Petri dish. Afterward, the cells were allowed to grow for further 24 h at 37 °C at 5% CO_2. Finally, the culture media were replaced with 3 mL of PBS and the Petri dish was mounted on the AFM stage immediately for the experiments. It needs to be pointed out that poly-L-Lysine is a biocompatible material that has been widely used for helping the adhesion of cells on the substrate in the AFM experiments and showed no obvious influence on cell viability.[18,40]

Force curves were acquired using the Dimension Edge instrument (Bruker Nano Surfaces, Santa Barbara, CA) in PBS buffer with commercial AFM probes (DNP-10). The probes were purchased from Bruker Corporation (Camarillo, CA) and their nominal spring constant was 0.06 N/m (according to manufacturer specifications). The spring constant of each probe used was calibrated against the stiff surface of Petri dish in PBS buffer by taking advantage of the thermal tune function contained in the AFM control software. The AFM system coupled with an optical microscope allowed to precisely locate the AFM tip on the central area of the cell. The force curves were taken at a velocity of 1 μm/s, with a threshold loading force of ~4.5 nN on each cell. The cell structure appeared unaffected under this threshold force because no abrupt drops or spikes were observed in the approach force curves. Previous studies showed that if a cell was penetrated by the AFM tip at high loading force, abrupt drops or spikes can be observed in the approach force curve.[41] At least 10 force curves were measured on each cell and more than 30 cells from five independent experiments were examined. The force−distance curves were obtained by correcting the cantilever bending by deducting the cantilever deflection from the z-piezo movement using a home-developed code written by Igor Pro (version 6.04, Wavemetrics Inc., Lake Oswego, OR). The zero point is the point at which the AFM cantilever begins to deflect upward. The mechanical property of the cells was quantitatively analyzed from the collected force−distance curves by the factor of viscosity,[17,18] which is defined by

$$\varphi = \text{viscous energy}/(\text{viscous energy} + \text{elastic energy}) \quad (2)$$

Self-developed Matlab-based procedures (version R2010a, Mathworks Inc., Natick, MA) were employed to carry out the calculations.

4.4. Comet Assay. HEK293T cells were seeded in 6-well plates (~3×10^5 cells/well, 3 mL/well) and cultured for 12 h at 37 °C at 5% CO_2, followed by the removal of the supernatant and washing of the cells with PBS twice (HyClone, Beijing, China). Afterward, the cells were exposed to culture media containing different concentrations of AgNPs (0, 10, 20, and 40 μg/mL) by adding 3 mL solution to each well. The cells were cultured for another 24 h at 37 °C at 5% CO_2. The supernatant was removed and the cells were washed with PBS twice. Afterward, the cells were collected into a centrifuge tube, centrifuged, washed once with, and resuspended into precooling PBS to a concentration of ~1×10^5 cells/mL for use in the following comet assay.

The comet assay is a widely accepted technique for detecting cellular DNA damages, and Trevigen Comet Assay Kit (Trevigen Inc., Gaithersburg, MD) was employed in the current study to measure the DNA damages by following the manufacturer's instructions. The procedures are very similar to our recent work.[8]

4.5. Gene Expression Profiling in HEK293T Cells. After treatment by AgNPs for 24 h, an RNAiso Plus reagent kit (Takara Biochemicals, Dalian, China) was used to extract RNAs from HEK293T cells cultured in 6-well plates according to the instruction provided by the manufacturer. The synthesis of cDNA was performed using the Primer Script RT reagent Kit (Takara Biochemicals, Dalian, China) under the guidance of the manufacturer's instructions. A SYBR Green RCR Kit (Toyobo, Tokyo, Japan) was used to carry out qRT-PCR experiments on an ABI 7300 System (PerkinElmer Applied Biosystems, Foster City, CA). The primers of target genes are listed in Table 3. All the samples were tested in triplicates and repeated three times independently. According to previous

Table 3. Primer Sequences Used for qRT-PCR

gene name	sequence of the primer (5′−3′)	product length
β-actin	F: CATGTACGTTGCTATCCAGGC	250
	R: CTCCTTAATGTCACGCACGAT	
Bcl2-t	F: AGAGTGCTGAAGATTGATGG	230
	R: ACTTGATTCTGGTGTTTCCC	
Bclw	F: GCCTTGTAGCCTTCTTTGTC	169
	R: GTATAGAGCTGTGAACTCCG	
Bid	F: GAGTGCATCACAAACCTACTG	198
	R: CTTGACTTTCAGAATCTGCCTC	

DOI: 10.1021/acsomega.8b00608
ACS Omega 2018, 3, 6770−6778

studies, β-actin mRNA was used as the internal control,[8,42] and the data of tested genes were normalized to β-actin mRNA by using the $2^{-\Delta\Delta CT}$ method. The expression alterations in mRNA induced by AgNPs are expressed in quantities relative to those of the control cells, correspondingly.

4.6. Statistical Analysis. The difference between the variables was evaluated by one-way analysis of variance followed by Dunnet test using SPSS17.0 software (SPSS Inc., Chicago, IL). Igor Pro (version 6.04, Wavemetrics Inc., Lake Oswego, OR) and Matlab (version R2010a, MathWorks Inc., Natick, NY) codes were written to extract the physical parameters from the force curves to obtain the factor of viscosity. The correlation between the factor of viscosity and the DNA damage was analyzed using Origin 8.5 software (OriginLab Co., Northampton, NY). The data are presented as mean ± standard error of mean. The statistical significance (p-value) between the control and experimental groups is denoted by * ($p < 0.05$), or ** ($p < 0.01$), or *** ($p < 0.001$).

AUTHOR INFORMATION

Corresponding Authors

*E-mail: peids@cigit.ac.cn (D.P.).
*E-mail: wanghuabin@citig.ac.cn (H.W.).

ORCID

Desheng Pei: 0000-0001-6408-9575
Huabin Wang: 0000-0001-5342-0672

Author Contributions

[‖]X.J. and C.L. contributed equally to this work.

Notes

The authors declare no competing financial interest.

ACKNOWLEDGMENTS

The authors are grateful for the supports from the National Natural Science Foundation of China (21407146, 21407145, and 11604332), the National Key Research and Development Program of China (2016YFC0101002, 2017YFF0106303, and 2016YFC0101301), the Central Government Supported Key Instrument Program of China (YXGYQ201700136), the Chinese Academy of Sciences (R52A500Z10), and Chongqing Science and Technology Commission (cstc2015jcyjiA10057, Y500061LH1, Y72Z530V10, cstccxljrc201714, cstc2014yykfC20004, and cstc2014yykfC20002).

REFERENCES

(1) Manke, A.; Wang, L. Y.; Rojanasakul, Y. Mechanisms of Nanoparticle-Induced Oxidative Stress and Toxicity. *BioMed Res. Int.* **2013**, *23*, No. 942916.

(2) Chaloupka, K.; Malam, Y.; Seifalian, A. M. Nanosilver as a New Generation of Nanoproduct in Biomedical Applications. *Trends Biotechnol.* **2010**, *28*, 580−588.

(3) Das, M.; Shim, K. H.; An, S. S. A.; Yi, D. K. Review on Gold Nanoparticles and their Applications. *Toxicol. Environ. Health Sci.* **2011**, *3*, 193−205.

(4) Li, Z.; Barnes, J. C.; Bosoy, A.; Stoddart, J. F.; Zink, J. I. Mesoporous Silica Nanoparticles in Biomedical Applications. *Chem. Soc. Rev.* **2012**, *41*, 2590−2605.

(5) Zhang, X. F.; Shen, W.; Gurunathan, S. Silver Nanoparticle-Mediated Cellular Responses in Various Cell Lines: An in Vitro Model. *Int. J. Mol. Sci.* **2016**, *17*, No. 1603.

(6) Schaeublin, N. M.; Braydich-Stolle, L. K.; Schrand, A. M.; Miller, J. M.; Hutchison, J.; Schlager, J. J.; Hussain, S. M. Surface Charge of Gold Nanoparticles Mediates Mechanism of Toxicity. *Nanoscale* **2011**, *3*, 410−420.

(7) Yang, X.; Liu, J. J.; He, H. W.; Zhou, L.; Gong, C. M.; Wang, X. M.; Yang, L. Q.; Yuan, J. H.; Huang, H. Y.; He, L. H.; Zhang, B.; Zhuang, Z. X. SiO2 Nanoparticles Induce Cytotoxicity and Protein Expression Alteration in HaCaT cells. *Part. Fibre Toxicol.* **2010**, *7*, No. 1.

(8) Lu, C. J.; Jiang, X. F.; Junaid, M.; Ma, Y. B.; Jia, P. P.; Wang, H. B.; Pei, D. S. Graphene Oxide Nanosheets Induce DNA Damage and Activate the Base Excision Repair (BER) Signaling Pathway both in Vitro and in Vivo. *Chemosphere* **2017**, *184*, 795−805.

(9) Zhang, X. F.; Choi, Y. J.; Han, J. W.; Kim, E.; Park, J. H.; Gurunathan, S.; Kim, J. H. Differential Nanoreprotoxicity of Silver Nanoparticles in Male Somatic Cells and Spermatogonial Stem Cells. *Int. J. Nanomed.* **2015**, *10*, 1335−1357.

(10) Wang, H.; Chen, L. G.; Sun, X. C.; Fu, A. L. Intracellular localisation of Proteins to Specific Cellular Areas by Nanocapsule Mediated Delivery. *J. Drug Targeting* **2017**, *25*, 724−733.

(11) Wang, J.; Deng, X. B.; Zhang, F.; Chen, D. L.; Ding, W. J. ZnO Nanoparticle-induced Oxidative Stress Triggers Apoptosis by Activating JNK Signaling Pathway in Cultured Primary Astrocytes. *Nanoscale. Res. Lett.* **2014**, *9*, No. 117.

(12) Zhu, B.; Li, Y. H.; Lin, Z. F.; Zhao, M. Q.; Xu, T. T.; Wang, C. B.; Deng, N. Silver Nanoparticles Induce HePG-2 Cells Apoptosis Through ROS-Mediated Signaling Pathways. *Nanoscale. Res. Lett.* **2016**, *11*, No. 198.

(13) Selim, M. E.; Hendi, A. A. Gold Nanoparticles Induce Apoptosis in MCF-7 Human Breast Cancer Cells. *Asian Pac. J. Cancer Prev.* **2012**, *13*, 1617−1620.

(14) Ahmad, J.; Ahamed, M.; Akhtar, M. J.; Alrokayan, S. A.; Siddiqui, M. A.; Musarrat, J.; Al-Khedhairy, A. A. Apoptosis Induction by Silica Nanoparticles Mediated through Reactive Oxygen Species in Human Liver Cell Line HepG2. *Toxicol. Appl. Pharmacol.* **2012**, *259*, 160−168.

(15) Wang, H.; Wilksch, J. J.; Lithgow, T.; Strugnell, R. A.; Gee, M. L. Nanomechanics Measurements of live Bacteria Reveal a Mechanism for Bacterial Cell Protection: The Polysaccharide Capsule in Klebsiella is a Responsive Polymer Hydrogel that Adapts to Osmotic Stress. *Soft Matter* **2013**, *9*, 7560−7567.

(16) Wang, H.; Wilksch, J. J.; Strugnell, R. A.; Gee, M. L. Role of Capsular Polysaccharides in Biofilm Formation: An AFM Nanomechanics Study. *ACS Appl. Mater. Interfaces* **2015**, *7*, 13007−13013.

(17) Wang, H.; Wilksch, J. J.; Chen, L. G.; Tan, J. W. H.; Strugnell, R. A.; Gee, M. L. Influence of Fimbriae on Bacterial Adhesion and Viscoelasticity and Correlations of the Two Properties with Biofilm Formation. *Langmuir* **2017**, *33*, 100−106.

(18) Yun, X. L.; Tang, M. J.; Yang, Z. B.; Wilksch, J. J.; Xiu, P.; Gao, H. Y.; Zhang, F.; Wang, H. B. Interrogation of Drug Effects on HeLa Cells by Exploiting New AFM Mechanical Biomarkers. *RSC Adv.* **2017**, *7*, 43764−43771.

(19) Zhang, B.; Li, L.; Li, Z. Q.; Liu, Y.; Zhang, H.; Wang, J. Z. Carbon Ion-Irradiated Hepatoma Cells Exhibit Coupling Interplay between Apoptotic Signaling and Morphological and Mechanical Remodeling. *Sci. Rep.* **2016**, *6*, No. 35131.

(20) Fang, Y.; Iu, C. Y.; Lui, C. N.; Zou, Y.; Fung, C. K.; Li, H. W.; Xi, N.; Yung, K. K.; Lai, K. W. Investigating Dynamic Structural and Mechanical Changes of Neuroblastoma Cells Associated with Glutamate-Mediated Neurodegeneration. *Sci. Rep.* **2014**, *4*, No. 7074.

(21) Dakal, T. C.; Kumar, A.; Majumdar, R. S.; Yadav, V. Mechanistic Basis of Antimicrobial Actions of Silver Nanoparticles. *Front. Microbiol.* **2016**, *7*, No. 1831.

(22) AshaRani, P. V.; Mun, G. L. K.; Hande, M. P.; Valiyaveettil, S. Cytotoxicity and Genotoxicity of Silver Nanoparticles in Human Cells. *ACS Nano* **2009**, *3*, 279−290.

(23) Foldbjerg, R.; Dang, D. A.; Autrup, H. Cytotoxicity and Genotoxicity of Silver Nanoparticles in the Human Lung Cancer Cell Line, A549. *Arch. Toxicol.* **2011**, *85*, 743−750.

(24) Sooklert, K.; Chattong, S.; Manotham, K.; Boonwong, C.; Klaharn, I. Y.; Jindatip, D.; Sereemaspun, A. Cytoprotective Effect of Gutaraldehyde Erythropoietin on HEK293 Kidney Cells after Silver Nanoparticle Exposure. *Int. J. Nanomed.* **2016**, *11*, 597−605.

DOI: 10.1021/acsomega.8b00608
ACS Omega 2018, 3, 6770−6778

(25) Ayllon, V.; Cayla, X.; Garcia, A.; Fleischer, A.; Rebollo, A. The Anti-apoptotic Molecules Bcl-X_L and Bcl-w Target Protein Phosphatase 1α to Bad. *Eur. J. Immunol.* **2002**, *32*, 1847−1855.
(26) Hu, X. L.; Olsson, T.; Johansson, I. M.; Brannstrom, T.; Wester, P. Dynamic Changes of the Anti- and Pro-apoptotic Proteins Bcl-w, Bcl-2, and Bax with Smac/Diablo Mitochondrial Release after Photothrombotic Ring Stroke in Rats. *Eur. J. Neurosci.* **2004**, *20*, 1177−1188.
(27) Lin, J.; Xu, H.; Wu, Y. Z.; Tang, M. J.; McEwen, G. D.; Liu, P.; Hansen, D. R.; Gilbertson, T. A.; Zhou, A. H. Investigation of Free Fatty Acid Associated Recombinant Membrane Receptor Protein Expression in HEK293 Cells Using Raman Spectroscopy, Calcium Imaging, and Atomic Force Microscopy. *Anal. Chem.* **2013**, *85*, 1374−1381.
(28) Luo, H.; Wang, F. F.; Bai, Y.; Chen, T. F.; Zheng, W. J. Selenium Nanoparticles Inhibit the Growth of HeLa and MDA-MB-231 Cells through Induction of S Phase Arrest. *Colloids Surf., B* **2012**, *94*, 304−308.
(29) Kaba, S. I.; Egorova, E. M. In Vitro Studies of the Toxic Effects of Silver Nanoparticles on HeLa and U937 Cells. *Nanotechnol., Sci. Appl.* **2015**, *8*, 19−29.
(30) Satapathy, S. R.; Mohapatra, P.; Preet, R.; Das, D.; Sarkar, B.; Choudhuri, T.; Wyatt, M. D.; Kundu, C. N. Silver-Based Nanoparticles Induce Apoptosis in Human Colon Cancer Cells Mediated through p53. *Nanomedicine* **2013**, *8*, 1307−1322.
(31) Ware, M. J.; Godin, B.; Singh, N.; Majithia, R.; Shamsudeen, S.; Serda, R. E.; Meissner, K. E.; Rees, P.; Summers, H. D. Analysis of the Influence of Cell Heterogeneity on Nanoparticle Dose Response. *ACS Nano* **2014**, *8*, 6693−6700.
(32) Kato, H. In vitro assays: Tracking Nanoparticles Inside Cells. *Nat. Nanotechnol.* **2011**, *6*, 139−140.
(33) Fritsch, A.; Höckel, M.; Kiessling, T.; Nnetu, K. D.; Wetzel, F.; Zink, M.; Käs, J. A. Are Biomechanical Changes Necessary for Tumour Progression? *Nat. Phys.* **2010**, *6*, 730−732.
(34) Di Carlo, D. A Mechanical Biomarker of Cell State in Medicine. *J. Lab. Autom.* **2012**, *17*, 32−42.
(35) Huang, Y.; Lu, X. Y.; Ma, J. W. Toxicity of Silver Nanoparticles to Human Dermal Fibroblasts on MicroRNA Level. *J. Biomed. Nanotechnol.* **2014**, *10*, 3304−3317.
(36) Piperakis, S. M.; Visvardis, E. E.; Tassiou, A. M. Comet Assay for Nuclear DNA Damage. *Methods Enzymol.* **1999**, *300*, 184−194.
(37) Sowmithra, K.; Shetty, N. J.; Jha, S. K.; Chaubey, R. C. Evaluation of Genotoxicity of the Acute Gamma Radiation on Earthworm Eisenia Fetida Using Single Cell Gel Electrophoresis Technique (Comet Assay). *Mutat. Res., Genet. Toxicol. Environ. Mutagen.* **2015**, *794*, 52−56.
(38) Rasool, E. A.; Abdul-Rasheed, O. F.; AL-Hashimi, A. F. Comparison between Different DNA and Conventional Sperm Parameters in Infertile Men. *Al-Kindy Col. Med. J.* **2012**, *8*, 40−47.
(39) Bhilwade, H. N.; Jayakumar, S.; Chaubey, R. C. Age-dependent Changes in Spontaneous Frequency of Micronucleated Erythrocytes in Bone Marrow and DNA Damage in Peripheral Blood of Swiss Mice. *Mutat. Res., Genet. Toxicol. Environ. Mutagen.* **2014**, *770*, 80−84.
(40) Ando, T.; Yonamoto, Y. In Situ EPR Detection of Reactive Oxygen Species in Adherent Cells Using Polylysine-coated Glass Plate. *Appl. Magn. Reson.* **2015**, *46*, 977−986.
(41) Vakarelski, I. U.; Brown, S. C.; Higashitani, K.; Moudgil, B. M. Penetration of Living Cell Membranes with Fortified Carbon Nanotube Tips. *Langmuir* **2007**, *23*, 10893−10896.
(42) Feng, D.; Witkowski, A.; Smith, S. Down-Regulation of Mitochondrial Acyl Carrier Protein in Mammalian Cells Compromises Protein Lipoylation and Respiratory Complex I and Results in Cell Death. *J. Biol. Chem.* **2009**, *284*, 11436−11445.

DOI: 10.1021/acsomega.8b00608
ACS Omega 2018, 3, 6770−6778